

In-orbit radiation damage characterization of SiPMs in GRID-02 CubeSat detector

Xutao Zheng^{a,b}, Huaizhong Gao^{a,b}, Jiaying Wen^{a,b}, Ming Zeng^{a,b,*}, Xiaofan Pan^{a,b}, Dacheng Xu^b, Yihui Liu^b, Yuchong Zhang^d, Haowei Peng^d, Yuchen Jiang^b, Xiangyun Long^{a,b}, Di'an Lu^b, Dongxin Yang^{a,b}, Hua Feng^{a,b,c}, Zhi Zeng^{a,b}, Jirong Cang^c, Yang Tian^{a,b}, GRID Collaboration

^a*Key Laboratory of Particle and Radiation Imaging (Tsinghua University), Ministry of Education, Beijing, 100084, People's Republic of China*

^b*Department of Engineering Physics, Tsinghua University, Beijing, 100084, People's Republic of China*

^c*Department of Astronomy, Tsinghua University, Beijing, 100084, People's Republic of China*

^d*Department of Physics, Tsinghua University, Beijing, 100084, People's Republic of China*

Abstract

Silicon photomultiplier (SiPM) has recently been used in several space-borne missions for scintillator readout, thanks to its solid state, compact size, low operating voltage and insensitivity to magnetic fields. However, a known issue of operating SiPM in space environment is the radiation damage and thus the performance degradation. In-orbit quantitative study of these effects is still very limited. In this work we present in-orbit SiPM characterization results obtained by the second detector of Gamma-Ray Integrated Detectors (GRID-02), which was launched on Nov. 6, 2020. An increase in dark current of $\sim 100 \mu\text{A}/\text{year}$ per SiPM chip (model MicroFJ-60035-TSV) at 28.5 V and 5°C is observed, and consequently the overall noise level (sigma) of GRID-02 detector increases $\sim 7.5 \text{ keV}/\text{year}$. The estimate of this increase is $\sim 50 \mu\text{A}/\text{year}$ per SiPM chip at -20°C, which indicates good effect of using a cooling system.

Keywords: SiPM, Radiation damage, Dark current, CubeSat, GRID

1. Introduction

Silicon photomultiplier (SiPM) has recently become popular photodetector for scintillator readout. Thanks to its compact size, solid state, low operating voltage and insensitivity to magnetic fields, SiPM has been a practical alternative to traditional photomultiplier tube (PMT), especially in space-borne applications. However, a known issue of SiPM is significant radiation damage and thus performance degradation caused by harsh space radiation environment.

*Corresponding author

Email address: zengming@tsinghua.edu.cn (Ming Zeng)

Table 1: Launched space missions utilizing SiPMs.

Project name	Launch date	Orbit	Ref.
Lazio-Sirad	2005.04.15	417 × 423 km 51.6° ISS	[1]
HXMT	2017.06.15	533 × 543 km 43.0° LEO	[2]
GRID-01	2018.10.29	502 × 519 km 97.4° LEO	[12]
SIRI-1	2018.12.03	567 × 589 km 97.7° SSO	[3, 4]
Mini-EUSO	2019.08.22	417 × 423 km 51.6° ISS	[6]
LabOSat	2020.01.15	Unknown LEO	[7]
GRID-02	2020.11.06	457 × 467 km 97.2° LEO	[12]
GECAM	2020.12.09	586 × 604 km 29.0° LEO	[8]
GRBAlpha	2021.03.22	534 × 563 km 97.5° LEO	[9]
SIRI-2	2021.12.07	35784 × 35788 km 0.0° GEO	[5]
GARI	2021.12.21	417 × 423 km 51.6° ISS	[11]
GRID-03B & GRID-04	2022.02.27	523 × 550 km 97.5° LEO	[12]

Several space missions utilizing SiPM have been launched so far as summarized in Table 1. Lazio-Sirad [1] studies the radiation environment inside International Space Station (ISS). The Hard X-ray Modulation Telescope (HXMT) [2] using SiPM in its automatic gain control system. SIRI-1 and SIRI-2 [3, 4, 5] aims to qualify new $\text{SrI}_2 : \text{Eu}$ scintillator and SiPM technology. Mini-EUSO [6] observes the Earth from ISS in UV range. LabOSat [7] is designed to technically validate SiPM with LEDs for excitation. Gravitational wave high-energy Electromagnetic Counterpart All-sky Monitor (GECAM) [8] is a mission composed of two small satellites to localize Gamma-Ray Bursts (GRBs) and its main detector, Gamma-Ray Detectors (GRDs), are based on $\text{LaBr}_3 : \text{Ce}$ and SiPM array. GRBAlpha [9], a 1U CubeSat mission, acts as the demonstration of CAMELOT [10], a fleet of CubeSats to observe GRBs. The GAGG Radiation Instruments (GARI) [11] are two identical instruments designed to space-qualify new gamma-ray detector technology for space-based astrophysical and defense applications. Gamma-Ray Integrated Detectors (GRID) [12] is a space mission concept with the purpose of monitor GRBs by a constellation of CubeSats equipped with GAGG:Ce scintillator and SiPM. The first GRID detector GRID-01 was launched on Oct. 29, 2018 and the subsequent one GRID-02 launched on Nov. 6, 2020. Other similar missions under development including: BurstCube [13], HERMES [14], EIRSAT-1 (GMOD) [15], Glowbug [16], CUBES [17], GALI [18].

In-orbit radiation damage effect studies of SiPM were hardly reported so far, although several experiments have been conducted at accelerator facilities [2, 19, 20, 21, 22]. SIRI-1 reports the only in-orbit result, which shows a significant increase in SiPM dark current [20]. In this article we present the in-orbit SiPM characterization results obtained by GRID-02 during the first few months after launch. Based on the basic measurement setups in the detector, we analyze the

change of breakdown voltage and dark current due to radiation damage. An estimate of dark current increasing rate of SiPM operating in LEO is given. The energy resolution and lower trigger threshold deterioration of GRID-02 as a result of dark count noise increase is also studied.

2. In-orbit characterization setup and methods

Besides the optimization for gamma-ray detection in GRID, several functions are specifically designed for performance study of SiPMs. The operating conditions, including current, bias voltage and temperature, of the SiPMs are monitored, and a charge injection module is used to analyze the noise contributions. Details about GRID instrument design could be found in [23]. Here we briefly review the biasing and readout circuits, and focus on the characterization setup.

The exploded view and a simplified block diagram of GRID detector are shown in Fig. 1 and Fig. 2. The detector comprises four independent channels designated as CH0 - CH3. Each channel consists of the scintillator crystal, the 4×4 array of MicroFJ-60035-TSV¹ SiPMs, the bias voltage power supply, the readout electronics, and the SiPM characterization circuits. A microcontroller (MCU) acts as control electronics, which monitors and controls the four channels.

Due to the limitation of power consumption and payload volume, there is no temperature control system in GRID detector. The temperature of GRID mainly depends on the overall temperature of the satellite. The temperature of each SiPM array is measured by a digital temperature sensor, TMP112², which offers 0.5°C accuracy.

Moreover, a charge injection module controlled by MCU is connected to the input of preamplifier so that a constant charge pulse could be injected at a specified frequency. Through charge injection with and without SiPM bias voltage, we are able to analyze the noise contributions, either from SiPM dark count noise or from electronics noise or other noise sources.

Figure 3 shows the schematic layout of $I \sim V$ measurement setup. The 16 SiPMs in the same array are simply connected in parallel, which means we can only characterize the whole array but not each single SiPM chips. The adjustable positive bias voltage on cathode is supplied by a switching regulator, LT3482³, and controlled by a 12-bit digital-to-analog converter (DAC), AD5672R⁴. After a resistive divider and a voltage follower, it is monitored by a MCU internal 12-bit analog-to-digital converter (ADC). The current through SiPMs is converted to voltage by a 1 kΩ grounding resistor on anode and measured by the same MCU internal ADC after a voltage follower. The difference

¹[MicroFJ-60035-TSV datasheet](#)

²[TMP112 datasheet](#)

³[LT3482 datasheet](#)

⁴[AD5672R datasheet](#)

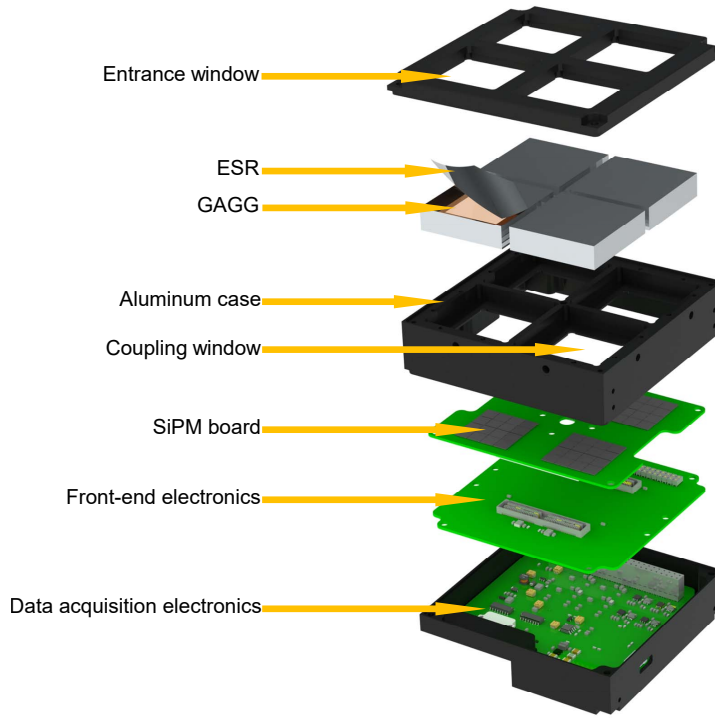


Figure 1: Exploded view of GRID detector. Details about GRID instrument design could be found in [23].

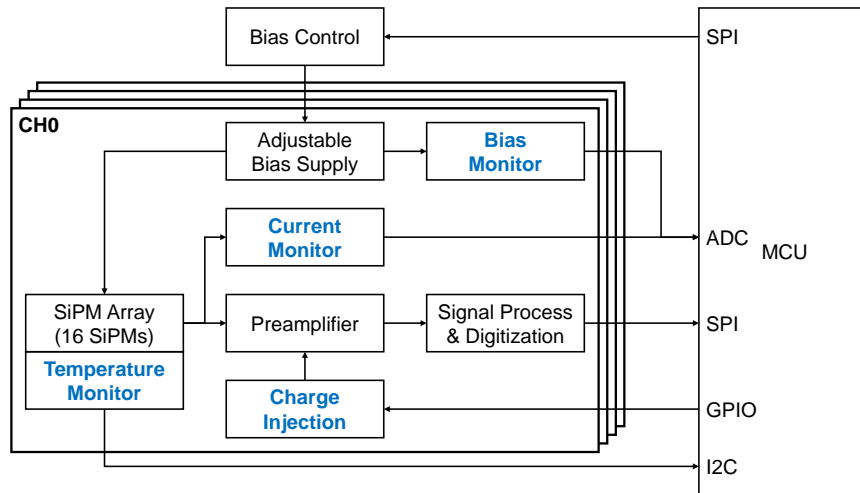


Figure 2: A simplified block diagram of GRID detector.

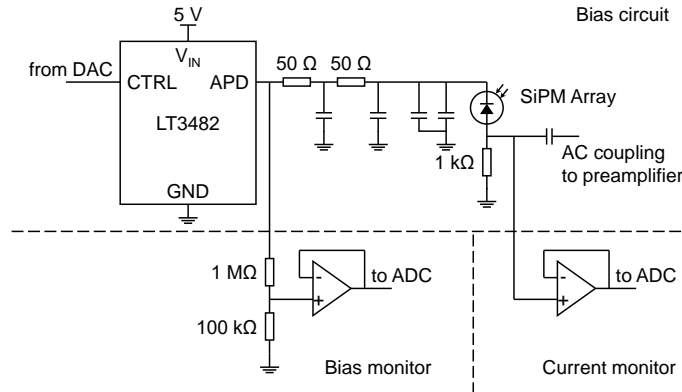


Figure 3: Schematic layout of $I \sim V$ measurement setup.

between these two voltages is the so-called bias voltage (V_{bias}) on SiPM. A proportional-integral-differential (PID) control method is applied to stabilize V_{bias} .

The current, bias voltage and temperature values are recorded as housekeeping data once per second during scientific observation, which is used to analyze SiPM dark current. Besides, the breakdown voltage (V_{bd}) of SiPM is determined by $I \sim V$ measurement at different bias voltages. This measurement method is encapsulated as a special mode triggered by an instruction. Once switched to this mode, the bias voltage will be successively changed to 40 preset values around and above V_{bd} . The measurement lasts for about 40 seconds, during which the temperature change is negligible. However, when compare between different measurements, temperature correction is performed.

Based on the characterization setup described above, we carefully scheduled characterization experiments and scientific observations. The payload debug phase began on Nov. 8, 2020 after launch and finished on Nov. 19, 2020. Then we moved to daily observation phase and arranged characterization experiments once per day since Dec. 4, 2020. Due to the existence of other payloads, the scientific observation time of GRID-02 is limited to about 20 ks (5 - 6 hours) per day.

3. Results

3.1. Breakdown voltage

Several methods could be used to extract V_{bd} from $I \sim V$ measurement, as well discussed in [24] and [25]. For convenience of comparison, the method mentioned in datasheet is applied [26]. The \sqrt{I} versus V_{bias} is linear fitted above V_{bd} and the V_{bd} is defined as the voltage intercept. Temperature correction is

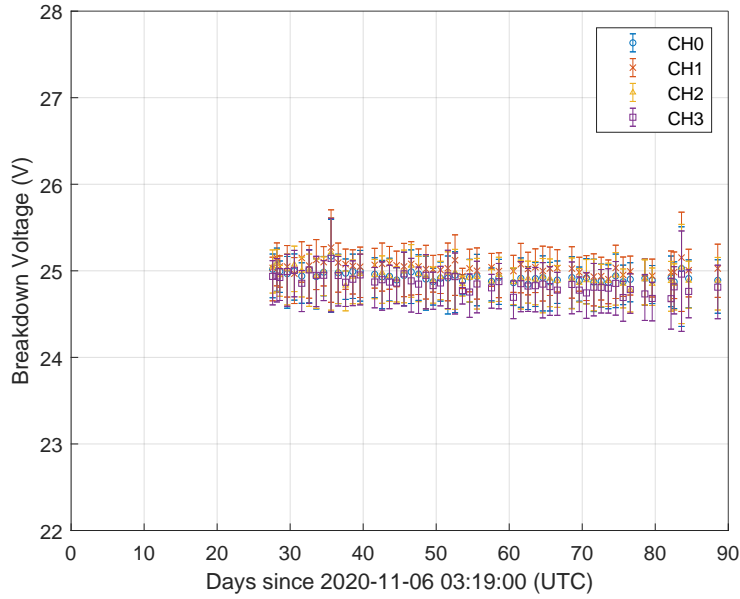


Figure 4: SiPM breakdown voltage (V_{bd}) as a function of time. The values are obtained by linear fit of \sqrt{I} versus bias voltage (V_{bias}) and corrected to 21°C.

adopted through

$$V_{bd}(T_{21}) = V_{bd}(T) - k_{bd} \cdot (T - T_{21}), \quad (1)$$

where $T_{21} = 21^\circ\text{C} = 294.15$ K is the standard measurement condition specified in datasheet, T is the absolute temperature of each $I \sim V$ measurement and $k_{bd} = 21.5$ mV/K is the temperature coefficient of V_{bd} specified in datasheet [26]. This k_{bd} value is also used in gain calibration procedure of GRID-02 [27]. In Fig. 4 we show V_{bd} as a function of time. V_{bd} has no obvious change in the error range. Other methods, such as polynomial fit of inverse logarithmic derivative ($ILD = (d \ln I / dV_{bias})^{-1}$), are going to be done in the future.

3.2. Dark current

The SiPM dark current (I_{dark}) could be expressed by

$$\begin{aligned} I_{dark} &= DCR \cdot (Gain \cdot e) \cdot ECF \\ &= DCR \cdot C_{pix} \cdot (V_{bias} - V_{bd}) \cdot ECF, \end{aligned} \quad (2)$$

where DCR is the dark count rate, $Gain$ the SiPM overall gain, e the elementary charge, ECF the excess charge factor and C_{pix} the pixel capacitance including

quenching capacitance [25]. The term $(V_{\text{bias}} - V_{\text{bd}})$ is also known as overvoltage (V_{ov}).

The C_{pix} is found independent of temperature or radiation damage [28] and the ECF which depends on V_{ov} is assumed approximately unchanged. The V_{bias} is set to 28.5 V without any temperature compensation so the temperature dependence of V_{bd} needs to be taken into account as discussed in section 3.1. Field-Enhanced Shockley-Read-Hall (FE-SRH) model [28, 29] indicates the relationship between DCR and temperature:

$$DCR(T) \propto \left(1 + 2\sqrt{3\pi} \frac{F_{\text{eff}}}{(kT)^{3/2}} e^{\left(\frac{F_{\text{eff}}}{(kT)^{3/2}}\right)^2} \right) T^2 e^{-\frac{E_a}{kT}}, \quad (3)$$

where F_{eff} is the effective electric field strength, k the Boltzmann constant and $E_a = 0.605$ eV the activation energy. Since V_{bias} is set to 28.5 V, F_{eff} is thought to remain unchanged.

Finally the I_{dark} expression becomes

$$I_{\text{dark}}(T) \propto \left(1 + 2\sqrt{3\pi} \frac{F_{\text{eff}}}{(kT)^{3/2}} e^{\left(\frac{F_{\text{eff}}}{(kT)^{3/2}}\right)^2} \right) T^2 e^{-\frac{E_a}{kT}} \cdot (V_{\text{bias}} - V_{\text{bd}}(T)). \quad (4)$$

We split data by date and assume that the radiation damage difference in the same day is negligible. Then we fit the plot of I_{dark} versus temperature with Eq. (4) and take F_{eff} as the free parameter. The I_{dark} values are unified to 5°C and shown in Fig. 5 as a function of time.

A linear fit shows that I_{dark} increases $\sim 93/96/98/110$ $\mu\text{A}/\text{year}$ per SiPM chip for CH0 - CH3 respectively, which is reasonably consistent with the result ~ 132 $\mu\text{A}/\text{year}$ per SiPM chip from SIRI-1 [20]. The difference among four channels might be caused by possible mechanical damage received before or during launch, while the difference between GRID-02 and SIRI-1 could be related to different orbit and different operating temperature. A discussion about dose difference is given in section 4.2.

We also extrapolate the fit of I_{dark} versus temperature to -20°C to evaluate those SiPMs working with cooling system. The increasing rate of I_{dark} at -20°C is ~ 50 $\mu\text{A}/\text{year}$ per SiPM chip, almost half of the value at 5°C .

3.3. Dark count noise

The energy resolution and noise contributions of the GRID detector is tested through charge injection. The charge injection peaks with and without bias voltage are fitted with Gauss functions to derive the standard deviation (σ) as shown in Fig. 6. Negative date values represent results obtained before launch. The error bars are within data points and therefore not shown for visualization purpose. The results in ADC channels are converted to equivalent energy with a scale factor ~ 0.027 keV/channel extracted from on-ground calibration data of GRID-02 [27]. Note that this value is heavily dependent on detector design, such as the electronics gain and the light yield of the scintillator crystal, so it is only applicable to GRID-02.

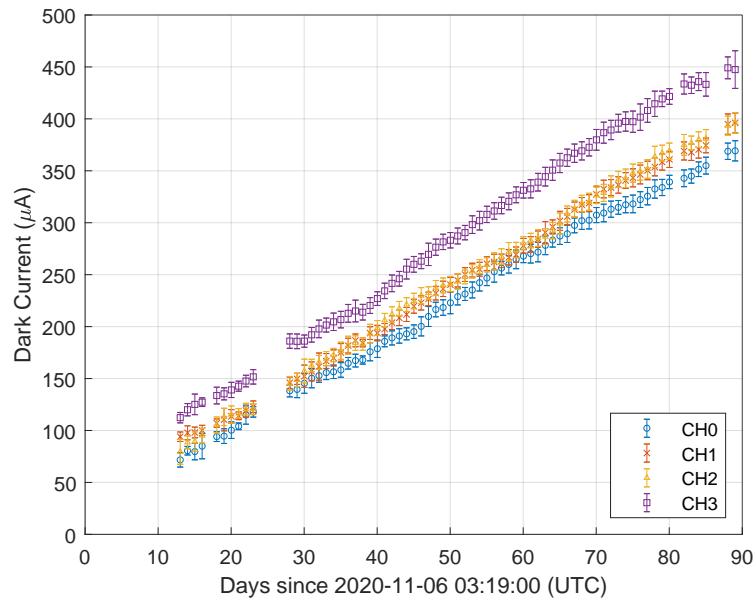


Figure 5: SiPM dark current (I_{dark}) at 28.5 V bias voltage as a function of time. The values are the sum of 16 SiPMs in the same channel and are unified to 5°C.

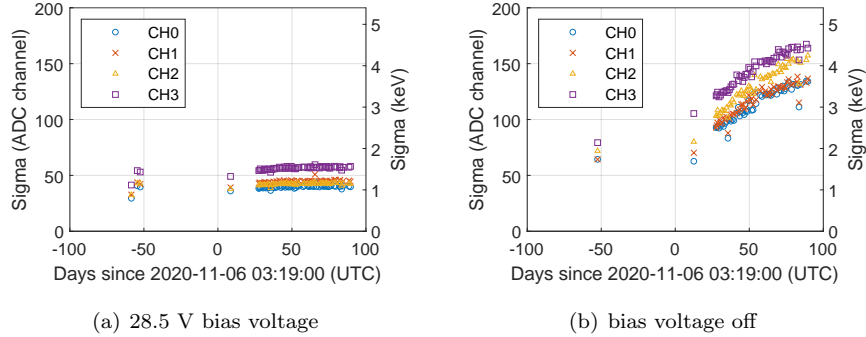


Figure 6: Standard deviation (σ) of charge injection peak as a function of time.

The σ_{elec} in Fig. 6(a) shows no significant change since it is dominated by electronics noise and fluctuation of injected charge itself. But, when bias power on and dark count noise becomes significant, σ_{total} gradually grows up with I_{dark} , as shown in Fig. 6(b). The total noise σ_{total} could be expressed by

$$\sigma_{\text{total}}^2 = \sigma_{\text{DC}}^2 + \sigma_{\text{elec}}^2, \quad (5)$$

where σ_{DC} is the dark current noise and Campbell's theorem shows its relationship with dark count rate (DCR) and I_{dark} :

$$\begin{aligned} \sigma_{\text{DC}}^2 &= DCR \cdot (Gain \cdot e)^2 \cdot \int h^2(t) dt \\ &\propto I_{\text{dark}} \cdot (V_{\text{bias}} - V_{\text{bd}}), \end{aligned} \quad (6)$$

where $h(t)$ is the unit impulse response of the readout electronics. Note that the I_{dark} here is the actual measurement result and should not be temperature corrected. In Fig. 7 we show the plot of σ_{total} versus I_{dark} and fit them with

$$\sigma_{\text{total}} = \sqrt{a_n \cdot I_{\text{dark}} \cdot (V_{\text{bias}} - V_{\text{bd}}) + b_n}, \quad (7)$$

where a_n and b_n are free parameters. The results indicate a noise increase of ~ 7.5 keV/year for each channel of GRID-02. The energy resolution and lower trigger threshold would grow up as well.

4. Discussions

4.1. Dark current estimation

Several previous studies found a linear relationship between I_{dark} and radiation damage measured by dose or particle fluences [2, 20, 28]. By simply assuming that radiation damage of SiPMs in GRID is linearly correlated with

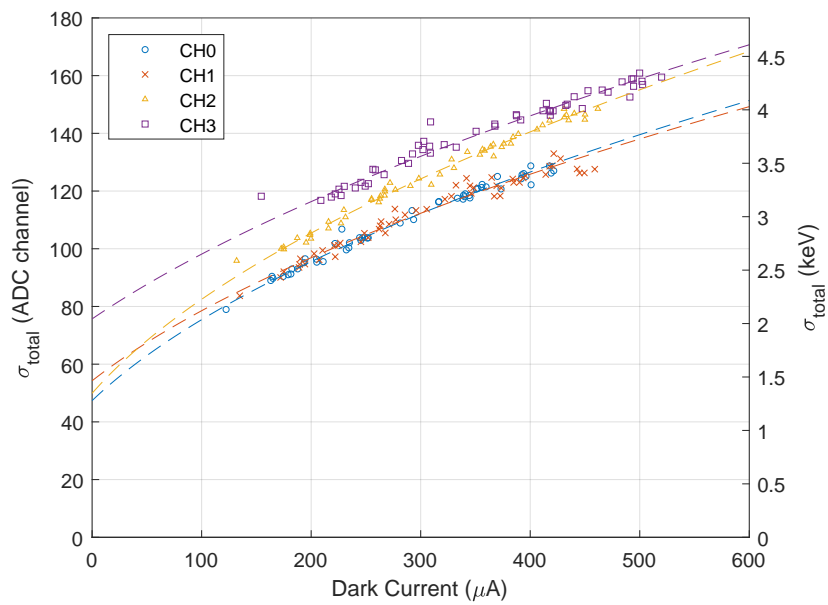


Figure 7: Detector total noise (σ_{total}) versus dark current (I_{dark}). The current are origin values without any correction.

Table 2: Fitting results of Eq. (8).

	a_{dc}	b_{dc}	$F_{\text{eff}}/k^{3/2}$
CH0	737.694	4236.96	10125.2
CH1	643.053	5100.42	10285.4
CH2	733.691	5298.48	10178.4
CH3	870.865	8744.55	10122.8

time, and the F_{eff} in Eq. (4) is independent of radiation damage, Eq. (4) is modified as

$$I_{\text{dark}}(\text{Time}, T) = (a_{\text{dc}} \cdot \text{Time} + b_{\text{dc}}) \cdot \left(1 + 2\sqrt{3\pi} \frac{F_{\text{eff}}}{(kT)^{3/2}} e^{\left(\frac{F_{\text{eff}}}{(kT)^{3/2}}\right)^2} \right) T^2 e^{-\frac{E_{\text{a}}}{kT}} \cdot (V_{\text{bias}} - V_{\text{bd}}(T)), \quad (8)$$

where a_{dc} , b_{dc} and F_{eff} are free parameters and Time is the days after launch. A joint fit of I_{dark} versus time and temperature gives the estimate of I_{dark} at specified conditions. The fitting results are listed in Table 2.

By substituting these parameters into Eq. (8), we obtain an approximate empirical equation around room temperature which describes the I_{dark} of GRID-02 at 28.5 V bias voltage, at specified time, and at specified temperature:

$$I_{\text{dark}}(\text{Time}, T) = 16 \cdot (0.26 \cdot \text{Time} + 1.96) \cdot e^{0.03428 \cdot (T - T_5)}, \quad (9)$$

where $T_5 = 5^\circ\text{C} = 278.15\text{ K}$ is the reference temperature of GRID-02. The unit of I_{dark} is μA and the first term 16 means the result is the sum of 16 SiPMs as in GRID detector. The exponential term shows that I_{dark} is doubled for $\sim 20^\circ\text{C}$ temperature increase.

4.2. Preliminary dose estimation

The radiation damage effect on SiPMs depends on irradiation particle type, energy and fluence and is traditionally evaluated by dose or 1 MeV neutron equivalent fluence [28]. In this paper we give an estimate of dose refer to the method used by SIRI-1 [20]. The SPENVIS online program [30] could generate particle flux with orbit information as listed in Table 1. The AP-8 and AE-8 (version solar minimum) trapped particle radiation models are selected for proton and electron, respectively. Then, with SHIELDOSE-2 model [31], SPENVIS calculates cumulative dose for a given period as shown in Fig. 8. The asymptotic value, $\sim 50\text{ rad(Si)}$, is used as an approximate estimate of dose. And the empirical equation of I_{dark} becomes

$$I_{\text{dark}}(\text{Dose}, T) = 16 \cdot (1.9 \cdot \text{Dose} + 1.96) \cdot e^{0.03428 \cdot (T - T_5)}, \quad (10)$$

where Dose is the cumulative dose in rad(Si) . We caution that this equation is applicable only when bias voltage is 28.5 V. Furthermore, detailed Monte

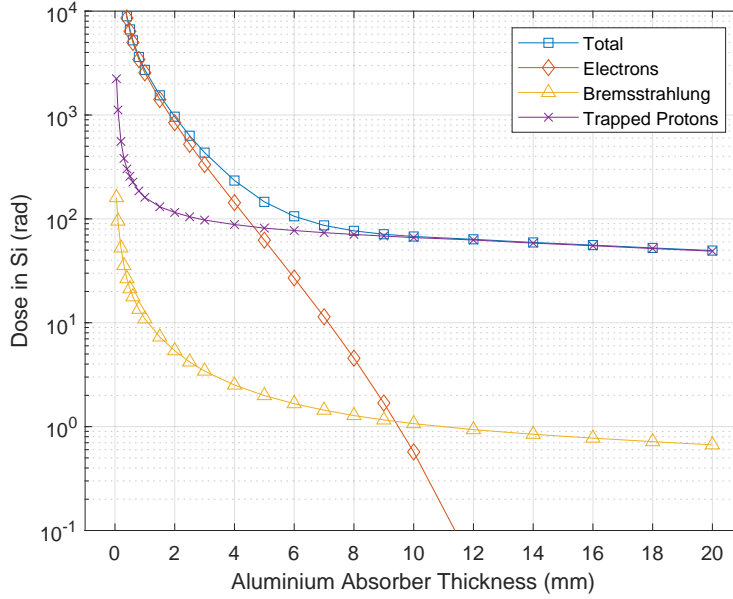


Figure 8: Annual dose in silicon as a function of aluminium shielding thickness for GRID-02 given by SHIELDOSE-2 from SPENVIS [30, 31]. Trapped radiation models for proton and electron are AP-8 and AE-8 (version solar minimum), respectively.

Carlo dose simulation could be done with the mass model of the satellite and the in-orbit radiation environment models.

To test this empirical equation, the dark current increasing rate calculated by Eq. (10) is compared with the measurement results of SIRI-1 and GRID-04, and they are in good accordance as listed in Table 3. This estimate of dark current can then be used with Eq. (7) to calculate noise increase and evaluate life span of the instrument. Note that the free parameters, a_n and b_n , in Eq. (7) is very dependent on readout electronics design, such as the readout time constant and the electronics gain. A ground calibration should be carried out to obtain these parameters.

4.3. Methods of improve signal-to-noise ratio

As discussed in section 3.3, the noise of radiation damaged SiPM is dominated by dark count noise described by Eq. (6). Here we give a discussion on qualitative methods of improve signal-to-noise ratio (SNR).

The first term is DCR which depends on temperature as shown in Eq. (3). This leads to a straight forward method which is lower the operating temperature. This might be difficult for CubeSats but is practicable for larger satellites.

Table 3: Measured and estimated dark current increasing rate of SIRI-1 and GRID-04.

Mission	Operating temperature (°C)	Operating voltage (V)	Orbit	Dose in silicon (rad)	Dark current increasing rate per SiPM chip ($\mu\text{A}/\text{year}$)	
					Measured	Estimated
SIRI-1	7.75	28.5	$567 \times 589 \text{ km } 97.7^\circ$	90	132	188
GRID-04	5	28.5	$523 \times 550 \text{ km } 97.5^\circ$	90	182	171

Fitting results in Table 2 gives a practical approximation that DCR reduced by half for 16°C temperature decrease around room temperature.

The second term is $Gain$ proportional to $V_{ov} = V_{bias} - V_{bd}$. As a critical operating parameter, the domino effect is enormous if V_{ov} is decreased. On one hand, noise reduces with decrease of $Gain$ and DCR . On the other hand, signal reduces as well due to decrease of $Gain$ and photon detection efficiency (PDE). Care must be taken to find the optimum value of V_{ov} .

The third term is the response of readout electronics. In general, shorter readout time constant leads to lower dark count noise. However, a too short readout time constant might cause problems such as larger ballistic deficit and more electronics noise. The lower limit is usually due to the scintillation decay time.

5. Conclusions

With the successful observation of several gamma ray bursts by GRID-02, the feasibility of SiPM in space application is once again proved. On the other hand, the significant radiation damage effect indicates the fact that life span evaluation requires more attention since the instrument design stage. As a CubeSat detector equipped with scintillator crystal and SiPM optimized for gamma-ray detection, GRID is specifically designed with SiPM characterization setups and conduct in-orbit characterization experiments. The characterization results of GRID-02 for the first few months show an increase in dark current of $\sim 100 \mu\text{A}/\text{year}$ per SiPM chip (model MicroFJ-60035-TSV) at 28.5 V and 5°C , which leads to the increase in overall noise level (sigma) of $\sim 7.5 \text{ keV}/\text{year}$. An approximate empirical equation around room temperature is given for dark current estimation at specified dose and temperature. The measured dark current of SIRI-1 and GRID-04 are used to test this equation and it shows a good agreement. This equation also implies that reduction of operating temperature could greatly mitigate the increase in dark current and noise which means a cooling system is highly recommended. Carefully designed readout electronics and optimum operating voltage help improve signal-to-noise ratio as well.

Acknowledgement

This work is supported by the Tsinghua University Initiative Scientific Research Program and the National Natural Science Foundation of China (Grant No. 11961141015). The authors would like to thank Dr. Shaolin Xiong and his colleagues of the GECAM satellite group from the IHEP of CAS, for open and fruitful discussions on topics related to this work.

References

- [1] R. Bencardino, F. Altamura, V. Bidoli, L. Bongiorno, M. Casolino, M. De Pascale, M. Ricci, P. Picozza, D. Aisa, A. Alvino, S. Ascani, P. Azzaarello, R. Battiston, S. Bizzaglia, M. Bizzarri, S. Blasko, L. Di Masso, G. Chiocci, D. Cosson, G. Esposito, S. Lucidi, A. Papi, V. Postolache, S. Rossi, G. Scolieri, M. Ionica, A. Franceschi, S. Dell’Agnello, C. Falcone, S. Tassa, A. Kalmikov, A. Popov, A. Abramov, M. Korotkov, A. Galper, A. Ivanova, L. Conti, V. Sgrigna, C. Stagni, A. Buzzi, D. Zilpimiani, A. Pontetti, L. Valentini, [Response of the LAZIO-SiRad detector to low energy electrons](#), in: 29th International Cosmic Ray Conference, ICRC 2005, Vol. 2, 2005, pp. 449–452.
URL <https://www.scopus.com/inward/record.uri?eid=2-s2.0-46149090466&partnerID=40&md5=661ca0afa31f4bd9fa0d662609d8fcce>
- [2] Z. Li, Y. Xu, C. Liu, Y. Gu, F. Xie, Y. Li, H. Hu, X. Zhou, X. Lu, X. Li, S. Zhang, Z. Chang, J. Zhang, Z. Xu, Y. Zhang, J. Zhao, [Characterization of radiation damage caused by 23 MeV protons in Multi-Pixel Photon Counter \(MPPC\)](#), Nuclear Instruments and Methods in Physics Research Section A: Accelerators, Spectrometers, Detectors and Associated Equipment 822 (2016) 63–70. doi:<https://doi.org/10.1016/j.nima.2016.03.092>.
URL <https://www.sciencedirect.com/science/article/pii/S016890021630122X>
- [3] L. J. Mitchell, B. F. Philips, R. S. Woolf, T. T. Finne, W. N. Johnson, E. G. Jackson, [Strontium Iodide Radiation Instrumentation \(SIRI\)](#), in: O. H. Siegmund (Ed.), UV, X-Ray, and Gamma-Ray Space Instrumentation for Astronomy XX, Vol. 10397, International Society for Optics and Photonics, SPIE, 2017, pp. 70 – 82. doi:[10.1117/12.2272606](https://doi.org/10.1117/12.2272606).
URL <https://doi.org/10.1117/12.2272606>
- [4] L. J. Mitchell, B. F. Philips, J. E. Grove, T. Finne, M. Johnson-Rambert, W. N. Johnson, [Strontium Iodide Radiation Instrument \(SIRI\) – Early On-Orbit Results](#) (2019). [arXiv:1907.11364](https://arxiv.org/abs/1907.11364).
- [5] L. J. Mitchell, B. F. Philips, R. S. Woolf, T. T. Finne, W. N. Johnson, [Strontium iodide radiation instrumentation II \(SIRI-2\)](#), in: O. H. Siegmund

- (Ed.), UV, X-Ray, and Gamma-Ray Space Instrumentation for Astronomy XXI, Vol. 11118, International Society for Optics and Photonics, SPIE, 2019, pp. 122 – 139. doi:[10.1117/12.2528073](https://doi.org/10.1117/12.2528073).
URL <https://doi.org/10.1117/12.2528073>
- [6] F. Capel, A. Belov, M. Casolino, P. Klimov, [Mini-EUSO: A high resolution detector for the study of terrestrial and cosmic UV emission from the International Space Station](#), Advances in Space Research 62 (10) (2018) 2954–2965, origins of Cosmic Rays. doi:<https://doi.org/10.1016/j.asr.2017.08.030>.
URL <https://www.sciencedirect.com/science/article/pii/S0273117717306257>
- [7] M. Barella, T. I. Burrioni, I. Carsen, M. Far, T. Ferreira Chase, L. Finazzi, F. Golmar, F. Gomez Marlasca, F. Izraelevitch, P. Levy, G. Sanca, [Silicon photomultiplier characterization on board a satellite in Low Earth Orbit](#), Nuclear Instruments and Methods in Physics Research Section A: Accelerators, Spectrometers, Detectors and Associated Equipment 979 (2020) 164490. doi:<https://doi.org/10.1016/j.nima.2020.164490>.
URL <https://www.sciencedirect.com/science/article/pii/S0168900220308871>
- [8] D. Zhang, X. Li, S. Xiong, Y. Li, X. Sun, Z. An, Y. Xu, Y. Zhu, W. Peng, H. Wang, F. Zhang, [Energy response of GECAM gamma-ray detector based on LaBr3:Ce and SiPM array](#), Nuclear Instruments and Methods in Physics Research Section A: Accelerators, Spectrometers, Detectors and Associated Equipment 921 (2019) 8–13. doi:<https://doi.org/10.1016/j.nima.2018.12.032>.
URL <https://www.sciencedirect.com/science/article/pii/S0168900218318291>
- [9] A. Pál, M. Ohno, L. Mészáros, N. Werner, J. Ripa, M. Frajt, N. Hirade, J. Hudec, J. Kapuš, M. Koleda, R. Laszlo, P. Lipovský, H. Mataka, M. Šmelko, N. Uchida, B. Csák, T. Enoto, Z. Frei, Y. Fukazawa, G. Galgóczi, K. Hirose, S. Hisadomi, Y. Ichinohe, L. L. Kiss, T. Mizuno, K. Nakazawa, H. Odaka, H. Takahashi, K. Torigoe, [GRBAlpha: a 1U CubeSat mission for validating timing-based gamma-ray burst localization](#), in: J.-W. A. den Herder, S. Nikzad, K. Nakazawa (Eds.), Space Telescopes and Instrumentation 2020: Ultraviolet to Gamma Ray, Vol. 11444, International Society for Optics and Photonics, SPIE, 2020, pp. 825 – 833.
URL <https://doi.org/10.1117/12.2561351>
- [10] N. Werner, J. Řípa, A. Pál, M. Ohno, N. Tarcai, K. Torigoe, K. Tanaka, N. Uchida, L. Mészáros, G. Galgóczi, Y. Fukazawa, T. Mizuno, H. Takahashi, K. Nakazawa, Z. Várhegyi, T. Enoto, H. Odaka, Y. Ichinohe, Z. Frei, L. Kiss, [CAMELOT: Cubesats Applied for MEasuring and Localising Transients mission overview](#), in: J.-W. A. den Herder, S. Nikzad,

- K. Nakazawa (Eds.), *Space Telescopes and Instrumentation 2018: Ultraviolet to Gamma Ray*, Vol. 10699, International Society for Optics and Photonics, SPIE, 2018, pp. 672 – 686.
 URL <https://doi.org/10.1117/12.2313764>
- [11] L. J. Mitchell, B. F. Philips, R. S. Woolf, T. T. Finne, A. L. Hutcheson, W. N. Johnson, M. Johnson-Rambert, R. Perea, *GAGG Radiation Instrumentation (GARI)*, in: O. H. Siegmund (Ed.), *UV, X-Ray, and Gamma-Ray Space Instrumentation for Astronomy XXII*, Vol. 11821, International Society for Optics and Photonics, SPIE, 2021, pp. 38 – 50.
 doi:[10.1117/12.2598588](https://doi.org/10.1117/12.2598588).
 URL <https://doi.org/10.1117/12.2598588>
- [12] J. Wen, X. Long, X. Zheng, Y. An, Z. Cai, J. Cang, Y. Che, C. Chen, L. Chen, Q. Chen, Z. Chen, Y. Cheng, L. Deng, W. Deng, W. Ding, H. Du, L. Duan, Q. Gan, T. Gao, Z. Gao, W. Han, Y. Han, X. He, X. He, L. Hou, F. Hu, J. Hu, B. Huang, D. Huang, X. Huang, S. Jia, Y. Jiang, Y. Jin, K. Li, S. Li, Y. Li, J. Liang, Y. Liang, W. Lin, C. Liu, G. Liu, M. Liu, R. Liu, T. Liu, W. Liu, D. Lu, P. Lu, Z. Lu, X. Luo, S. Ma, Y. Ma, X. Mao, Y. Mo, Q. Nie, S. Qu, X. Shan, G. Shi, W. Song, Z. Sun, X. Tan, S. Tang, M. Tao, B. Wang, Y. Wang, Z. Wang, Q. Wu, X. Wu, Y. Xia, H. Xiao, W. Xie, D. Xu, R. Xu, W. Xu, L. Yan, S. Yan, D. Yang, H. Yang, H. Yang, Y.-S. Yang, Y. Yang, L. Yao, H. Yu, Y. Yu, A. Zhang, B. Zhang, L. Zhang, M. Zhang, S. Zhang, T. Zhang, Y. Zhang, Q. Zhao, R. Zhao, S. Zheng, X. Zhou, R. Zhu, Y. Zou, P. An, Y. Cai, H. Chen, Z. Dai, Y. Fan, C. Feng, H. Feng, H. Gao, L. Huang, M. Kang, L. Li, Z. Li, E. Liang, L. Lin, Q. Lin, C. Liu, H. Liu, X. Liu, Y. Liu, X. Lu, S. Mao, R. Shen, J. Shu, M. Su, H. Sun, P.-H. Tam, C.-P. Tang, Y. Tian, F. Wang, J. Wang, W. Wang, Z. Wang, J. Wu, X. Wu, S. Xiong, C. Xu, J. Yu, W. Yu, Y. Yu, M. Zeng, Z. Zeng, B.-B. Zhang, B. Zhang, Z. Zhao, R. Zhou, Z. Zhu, *GRID: a student project to monitor the transient gamma-ray sky in the multi-messenger astronomy era*, *Experimental Astronomy* 48 (2019) 77–95. doi:<https://doi.org/10.1007/s10686-019-09636-w>.
 URL <https://link.springer.com/article/10.1007/s10686-019-09636-w>
- [13] J. Racusin, J. S. Perkins, M. S. Briggs, G. de Nolfo, J. Krizmanic, R. Caputo, J. E. McEnery, P. Shawhan, D. Morris, V. Connaughton, D. Kocevski, C. Wilson-Hodge, M. Hui, L. Mitchell, S. McBreen, *BurstCube: A CubeSat for Gravitational Wave Counterparts* (2017). [arXiv:1708.09292](https://arxiv.org/abs/1708.09292).
- [14] F. Fuschino, R. Campana, C. Labanti, Y. Evangelista, M. Feroci, L. Burderi, F. Fiore, F. Ambrosino, G. Baldazzi, P. Bellutti, R. Bertacini, G. Bertuccio, G. Borghi, D. Cirrincione, D. Cauz, F. Ficorella, M. Fiorini, M. Gandola, M. Grassi, A. Guzman, G. L. Rosa, M. Lavagna, P. Lunghi, P. Malcovati, G. Morgante, B. Negri, G. Pauletta, R. Pizzolla, A. Picciotto, S. Pirrotta, S. Pliego-Caballero, S. Puccetti,

- A. Rachevski, I. Rashevskaya, L. Rignanese, M. Salatti, A. Santangelo, S. Silvestrini, G. Sottile, C. Tenzer, A. Vacchi, G. Zampa, N. Zampa, N. Zorzi, [HERMES: An ultra-wide band X and gamma-ray transient monitor on board a nano-satellite constellation](#), Nuclear Instruments and Methods in Physics Research Section A: Accelerators, Spectrometers, Detectors and Associated Equipment 936 (2019) 199–203, frontier Detectors for Frontier Physics: 14th Pisa Meeting on Advanced Detectors. doi:<https://doi.org/10.1016/j.nima.2018.11.072>.
URL <https://www.sciencedirect.com/science/article/pii/S0168900218316814>
- [15] D. Murphy, J. Mangan, A. Ulyanov, S. Walsh, R. Dunwoody, L. Hanlon, B. Shortt, S. McBreen, [Balloon flight test of a CeBr₃ detector with silicon photomultiplier readout](#), Experimental Astronomy 52 (2021) 1–34. doi:<https://doi.org/10.1007/s10686-021-09767-z>.
URL <https://link.springer.com/article/10.1007/s10686-021-09767-z>
- [16] G. J.E., C. C.C., K. M., M. L.J., P. B.F., W. R.S., W. E., W.-H. C.A., K. D., B. M.S., P. J., G. S., H. D., [Glowbug, a gamma-ray telescope for bursts and other transients](#), AAS/High Energy Astrophysics Division, AAS/High Energy Astrophysics Division (2019) 109.52.
URL <https://www.scopus.com/inward/record.uri?eid=2-s2.0-85083912941&partnerID=40&md5=a2611321cc5db0b8a44cab8eddb6ea87>
- [17] R. Kushwah, T. Stana, M. Pearce, [The design and performance of CUBES — a CubeSat x-ray detector](#), Journal of Instrumentation 16 (08) (2021) P08038. doi:[10.1088/1748-0221/16/08/p08038](https://doi.org/10.1088/1748-0221/16/08/p08038).
URL <https://doi.org/10.1088/1748-0221/16/08/p08038>
- [18] R. Rahin, L. Moleri, A. Vdovin, A. Feigenboim, S. Margolin, S. Tarem, E. Behar, M. Ghelman, A. Osovizky, [GALI: a gamma-ray burst localizing instrument](#), in: J.-W. A. den Herder, S. Nikzad, K. Nakazawa (Eds.), Space Telescopes and Instrumentation 2020: Ultraviolet to Gamma Ray, Vol. 11444, International Society for Optics and Photonics, SPIE, 2020, pp. 1037 – 1049. doi:[10.1117/12.2576126](https://doi.org/10.1117/12.2576126).
URL <https://doi.org/10.1117/12.2576126>
- [19] K. Bartlett, D. Coupland, D. Beckman, K. Mesick, [Proton irradiation damage and annealing effects in on semiconductor j-series silicon photomultipliers](#), Nuclear Instruments and Methods in Physics Research Section A: Accelerators, Spectrometers, Detectors and Associated Equipment 969 (2020) 163957. doi:<https://doi.org/10.1016/j.nima.2020.163957>.
URL <https://www.sciencedirect.com/science/article/pii/S0168900220304289>

- [20] L. Mitchell, B. Philips, W. N. Johnson, M. Johnson-Rambert, A. N. Kansky, R. Woolf, [Radiation damage assessment of SensL SiPMs](#), Nuclear Instruments and Methods in Physics Research Section A: Accelerators, Spectrometers, Detectors and Associated Equipment 988 (2021) 164798. doi:<https://doi.org/10.1016/j.nima.2020.164798>. URL <https://www.sciencedirect.com/science/article/pii/S0168900220311955>
- [21] N. Hirade, H. Takahashi, N. Uchida, M. Ohno, K. Torigoe, Y. Fukazawa, T. Mizuno, H. Mataka, K. Hirose, S. Hisadomi, K. Nakazawa, K. Yamaoka, N. Werner, J. Rípa, S. Hatori, K. Kume, S. Mizushima, [Annealing of proton radiation damages in si-pm at room temperature](#), Nuclear Instruments and Methods in Physics Research Section A: Accelerators, Spectrometers, Detectors and Associated Equipment 986 (2021) 164673. doi:<https://doi.org/10.1016/j.nima.2020.164673>. URL <https://www.sciencedirect.com/science/article/pii/S0168900220310706>
- [22] A. Ulyanov, D. Murphy, J. Mangan, V. Gupta, W. Hajdas, D. de Faote, B. Shortt, L. Hanlon, S. McBreen, [Radiation damage study of sensl j-series silicon photomultipliers using 101.4 mev protons](#), Nuclear Instruments and Methods in Physics Research Section A: Accelerators, Spectrometers, Detectors and Associated Equipment 976 (2020) 164203. doi:<https://doi.org/10.1016/j.nima.2020.164203>. URL <https://www.sciencedirect.com/science/article/pii/S0168900220305994>
- [23] J.-X. Wen, X.-T. Zheng, J.-D. Yu, Y.-P. Che, D.-X. Yang, H.-Z. Gao, Y.-F. Jin, X.-Y. Long, Y.-H. Liu, D.-C. Xu, Y.-C. Zhang, M. Zeng, Y. Tian, H. Feng, Z. Zeng, J.-R. Cang, Q. Wu, Z.-Q. Zhao, B.-B. Zhang, P. An, [Compact CubeSat Gamma-ray detector for GRID mission](#), Nuclear Science and Techniques 32 (2021) 99. doi:<https://doi.org/10.1007/s41365-021-00937-4>. URL <https://link.springer.com/article/10.1007/s41365-021-00937-4>
- [24] F. Nagy, G. Hegyesi, G. Kalinka, J. Molnár, [A model based DC analysis of SiPM breakdown voltages](#), Nuclear Instruments and Methods in Physics Research Section A: Accelerators, Spectrometers, Detectors and Associated Equipment 849 (2017) 55–59. doi:<https://doi.org/10.1016/j.nima.2017.01.002>. URL <https://www.sciencedirect.com/science/article/pii/S0168900217300025>
- [25] R. Klanner, [Characterisation of SiPMs](#), Nuclear Instruments and Methods in Physics Research Section A: Accelerators, Spectrometers, Detectors and Associated Equipment 926 (2019) 36–56, silicon Photomultipliers: Technology, Characterisation and Applications.

- doi:<https://doi.org/10.1016/j.nima.2018.11.083>.
URL <https://www.sciencedirect.com/science/article/pii/S0168900218317091>
- [26] Datasheet: Silicon Photomultipliers (SiPM), High PDE and Timing Resolution Sensors in a TSV Package (2021).
URL <https://www.onsemi.com/pdf/datasheet/microj-series-d.pdf>
- [27] H. Gao, D. Yang, J. Wen, X. Zheng, M. Zeng, J. Cang, W. Zeng, X. Pan, Q. Zhou, Y. Liu, H. Feng, B. Zhang, Z. Zeng, Y. Tian, G. Collaboration, [On-ground calibrations of the GRID-02 gamma-ray detector](#), *Experimental Astronomy* 53 (2021) 103–116. doi:<https://doi.org/10.1007/s10686-021-09819-4>.
URL <https://link.springer.com/article/10.1007/s10686-021-09819-4>
- [28] E. Garutti, Y. Musienko, [Radiation damage of SiPMs](#), *Nuclear Instruments and Methods in Physics Research Section A: Accelerators, Spectrometers, Detectors and Associated Equipment* 926 (2019) 69–84, silicon Photomultipliers: Technology, Characterisation and Applications. doi:<https://doi.org/10.1016/j.nima.2018.10.191>.
URL <https://www.sciencedirect.com/science/article/pii/S0168900218315055>
- [29] G. Hurkx, H. de Graaff, W. Kloosterman, M. Knuvers, A new analytical diode model including tunneling and avalanche breakdown, *IEEE Transactions on Electron Devices* 39 (9) (1992) 2090–2098. doi:[10.1109/16.155882](https://doi.org/10.1109/16.155882).
- [30] ESA, [SPace ENVironment Information System \(SPENVIS\)](#), Online (1997-2022).
URL <https://www.spennis.oma.be/>
- [31] S. Seltzer, [Updated Calculations for Routine Space-Shielding Radiation Dose Estimates: SHIELDOSE-2](#) (1994).
URL https://tsapps.nist.gov/publication/get_pdf.cfm?pub_id=103635